

# Polymers End-Grafted onto a Cylindrical Surface

Michael Murat<sup>†</sup> and Gary S. Grest\*

Corporate Research Science Laboratories, Exxon Research and Engineering Company, Annandale, New Jersey 08801

Received June 15, 1990

**ABSTRACT:** Equilibrium properties of linear polymers grafted at one end onto a repulsive cylindrical surface of radius  $R$  are studied by using molecular dynamics simulations.  $R$  is varied between the limiting cases of a flat surface ( $R \rightarrow \infty$ ) and a grafting line ( $R = 0$ ). Polymers consisting of 50–150 monomers are grafted randomly at an average surface coverage of  $\rho_a$  onto a cylindrical surface immersed in a good solvent.  $\rho_a$  is taken to be large enough to induce overlap and consequent stretching of the chains. We present results for the monomer density profile and the density of the free ends. We find no evidence for the existence of a dead zone near the surface from which the free ends are excluded in any of the systems with finite  $R$ . This is in contrast with some recent predictions that such a dead zone should exist in the case of polymers in a melt state, and probably under good solvent conditions as well. Only when  $R \rightarrow 0$  (that is, polymers grafted on a line) do we see an indication of a dead zone.

## I. Introduction

Recently there has been an increased interest in the structure of polymers grafted onto a flat surface (the so-called "brushes"). Following the theoretical works of Alexander<sup>1</sup> and de Gennes,<sup>2,3</sup> who used a scaling approach, different techniques were applied to the study of these systems. Monte Carlo and numerical self-consistent-field (SCF) calculations were performed by Cosgrove et al.,<sup>4</sup> resulting in a monomer density profile different from the uniform one assumed by the earlier studies. Later, Milner et al.<sup>5,6</sup> treated the "classical" limit of strongly stretched chains using SCF theory, as first discussed by Semenov<sup>7</sup> in a different context. They solved the SCF equations analytically for very high molecular weight and obtained a parabolic density profile. Another interesting result of these calculations is that the free ends could explore all the space within the brush, even very close to the grafting surface, where the monomer density is high. This lack of a "dead zone", from which the ends would be excluded, is a remarkable prediction of the theory, which is not easy to verify experimentally. Later, molecular dynamics<sup>8</sup> and Monte Carlo<sup>9</sup> simulations were carried out to study polymer brushes in detail. These studies confirmed the existence of a parabolic density profile for a certain range of surface coverages, as well as the absence of a dead zone. A numerical solution of the SCF equations by Skvortsov et al.,<sup>10</sup> carried out independently of the work of Milner et al., also obtained very similar predictions. Experimental neutron-scattering studies<sup>11</sup> of end-grafted polymers are also consistent with a parabolic density profile.

A natural extension of these studies is the case of polymers grafted onto a curved surface. Experimental realizations of such systems can occur when polymers are attached to spherical colloidal particles for purposes of colloidal stabilization or when they are grafted onto cylindrical mica surfaces for the study of the interactions between brushes.<sup>12,13</sup> Recently, the SCF theory has been applied to convex (spherical and cylindrical) surfaces by Ball et al.<sup>14</sup> For the cylindrical case under melt conditions, it is found that the free ends are excluded from a zone near the grafting surface. The thickness of this dead zone varies between zero for a flat surface to a finite fraction of the brush height,  $h$ , in the limit of strong curvature, when  $R/h$  is of order unity. Although this system, which

corresponds to a uniform monomer density up to the brush height, is of interest by itself, one would like to understand the situation in an experimentally more realistic case, that of, a brush in good solvent conditions. This case has proven to be more difficult to treat and has not yet been solved. However, on the basis of the earlier work of Milner and Witten<sup>15</sup> on the bending moduli of polymeric interfaces, Ball et al.<sup>14</sup> suggest that such an exclusion zone would also appear for the good solvent case, even for large radii of curvature.

Such exclusion zones have been observed in a special limiting case of grafted polymers, namely, star polymers. These consist of  $f$  chains of length  $N$  attached on one of their ends to a common point. Daoud and Cotton<sup>16</sup> showed that under good solvent conditions and in the limit of large  $f$  and  $N$ , the monomer density as a function of the distance from the center should fall off as  $\rho(r) \propto f^{2/3}r^{-4/3}$ . Because of such high densities near the center, the free ends of the chains are pushed outward. Simulating this system by a molecular dynamics method, Grest et al.<sup>17</sup> found that the distribution of center-end distances is Gaussian, with a width much smaller than the average center-end distance. Thus for this case, the dead zone extends to a finite fraction of the star's radius.

In this report, we study systems of cylindrical brushes under good solvent conditions with varying radii of curvature and surface coverage and address the question of the existence of the exclusion zone using a molecular dynamics simulation. We find that the monomer density profile changes from a parabolic form to a more rapidly decaying one as the radius of curvature,  $R$ , of the grafting cylinder is reduced. We find no evidence of a dead zone for any finite  $R$ . An indication of a dead zone is observed when the cylinder is reduced to a single line. While this limiting case has been treated previously<sup>18</sup> by using a scaling theory, no previous simulations have been performed in this limit. We extend our simulations to cover this regime as well.

In the next section we describe our simulation method and give details of the model systems studied. Section III describes the results of our simulation for systems at a constant surface coverage and finite values of  $R/h$ . In section IV we treat the limiting case of polymers grafted on a thin line ( $R = 0$ ). Finally in section V we summarize our results.

<sup>†</sup> Present address: Soreq Nuclear Research Center, Yavne 70600, Israel.

**Table I**  
**Properties of the Systems Studied for the Case of Polymers Grafted onto a Cylinder of Radius  $R^a$**

| $N$ | $\rho_a$ | $R$ | $T_t/\tau$ | $\langle d \rangle$ | $\langle d_e \rangle$ | $\langle R_G^2 \rangle$ | $\langle R_{G_{\perp}}^2 \rangle$ |
|-----|----------|-----|------------|---------------------|-----------------------|-------------------------|-----------------------------------|
| 150 | 0.03     | 2   | 6000       | 18.0                | 28.3                  | 121.7                   | 96.6                              |
| 100 | 0.03     | 2   | 12000      | 11.3                | 17.1                  | 61.2                    | 45.2                              |
| 50  | 0.03     | 2   | 3000       | 7.0                 | 10.7                  | 24.6                    | 17.9                              |
| 50  | 0.03     | 5   | 6000       | 7.2                 | 11.1                  | 25.9                    | 19.3                              |
| 50  | 0.03     | 20  | 3000       | 7.6                 | 11.7                  | 27.4                    | 21.2                              |
| 50  | 0.1      | 5   | 6000       | 9.2                 | 14.6                  | 30.9                    | 25.8                              |
| 50  | 0.2      | 5   | 6000       | 11.0                | 17.8                  | 38.2                    | 33.8                              |

<sup>a</sup> Here  $N$  is the chain length,  $\rho_a$  is the surface coverage,  $T_t$  is the total duration of the run (after equilibration),  $\langle d \rangle$  is the average height of the monomers from the cylinder surface,  $\langle d_e \rangle$  is the average height of the free ends from the cylinder surface,  $\langle R_G^2 \rangle$  is the average radius of gyration of the chains squared, and  $\langle R_{G_{\perp}}^2 \rangle$  is the sum of the contributions to the average radius of gyration squared in the directions perpendicular to the cylinder axis.

## II. Method

We studied systems of cylindrical surfaces of radius  $R$  onto which  $M$  polymers of  $N + 1$  monomers are anchored at one end. Each plate has a surface area  $S = 2\pi Rl_x$ , giving a grafting density of  $\rho_a = M/S$ .  $l_x$  is the length of the cylinder in the  $x$ -direction, in which periodic boundary conditions are used. The first monomer of each chain is placed at a random position on the cylinder while the remaining  $N$  are initially radially extended. The system was then equilibrated by using the molecular dynamics method described below. The equilibration was carried out much longer than the relaxation time of the individual chains, calculated by using the procedure described previously.<sup>8</sup> After equilibration, the simulation was continued and the configurations of the chains saved at prescribed intervals to calculate the quantities of interest later. The limiting case of polymers grafted on a line is simulated by using the same technique but taking  $R$  to be very small. In this case, instead of  $\rho_a$ , it is more appropriate to define a line density  $\rho_l = M/l_x$ .

The simulations are performed by using a molecular dynamics method in which each monomer is coupled to a heat bath.<sup>19</sup> This method has already been successfully applied to several problems related to static and dynamic properties of polymers<sup>19-21</sup> and of polymeric membranes.<sup>22</sup> The monomers are treated as beads of mass  $m$ , which interact through a shifted short-range Lennard-Jones potential given by

$$U^0(r) = \begin{cases} 4\epsilon \left[ \left( \frac{\sigma}{r} \right)^{12} - \left( \frac{\sigma}{r} \right)^6 + \frac{1}{4} \right] & \text{if } r \leq r_c \\ 0 & r > r_c \end{cases} \quad (1)$$

with  $r_c = 2^{1/6}\sigma$ . As this potential is purely repulsive, our simulations are in a good solvent regime. In addition, there is an attractive interaction between neighboring monomers along the chains and a strongly repulsive one of range  $\sigma/2$  between the wall and the monomers. Parameters of these potentials are the same as in ref 8. Denoting the total potential of monomer  $i$  by  $U_i$ , the equation of motion for monomer  $i$  is given by

$$m \frac{d^2 \vec{r}_i}{dt^2} = -\vec{\nabla} U_i - m\Gamma \frac{d\vec{r}_i}{dt} + \vec{W}_i(t) \quad (2)$$

Here  $\Gamma$  is the bead friction, which acts to couple the monomers to the heat bath.  $\vec{W}_i(t)$  describes the random force acting on each bead. It can be written as a Gaussian white noise with

$$\langle \vec{W}_i(t) \cdot \vec{W}_j(t') \rangle = 6k_B T m \Gamma \delta_{ij} \delta(t-t') \quad (3)$$

where  $T$  is the temperature and  $k_B$  is the Boltzmann constant. We have used  $\Gamma = 0.5\tau^{-1}$  and  $k_B T = 1.2\epsilon$ . Here  $\tau = \sigma(m/\epsilon)^{1/2}$  is the natural time unit for such a system. With this choice of parameters, the average bond length between neighboring beads along the chains is found to be  $0.97\sigma$ . The equations of motion are then solved by using a predictor-corrector algorithm with a time step  $\Delta t = 0.006\tau$ . The total length of the runs  $T_t/\tau$  (after equilibration) is presented in Tables I and II for all of the cases studied.

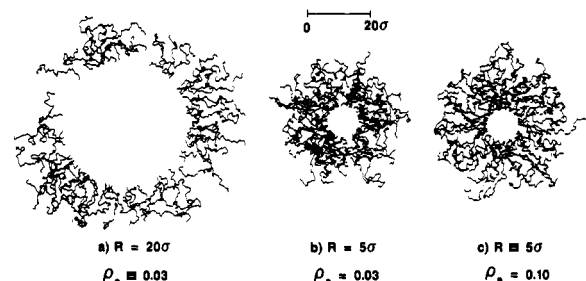
## III. Surfaces with Finite $R$

Figure 1 shows a typical configuration for three of the systems studied. The chains are projected onto the plane perpendicular to the axis of the grafting cylinder. Each

**Table II**  
**Properties of the Systems Studied in the Case of Polymers Grafted onto a Grafting Line at a Line Density of  $\rho_l^a$**

| $N$ | $\rho_l$ | $T_t/\tau$ | $\langle d \rangle$ | $\langle d_e \rangle$ | $\langle R_G^2 \rangle$ | $\langle R_{G_{\perp}}^2 \rangle$ |
|-----|----------|------------|---------------------|-----------------------|-------------------------|-----------------------------------|
| 50  | 0.38     | 2400       | 7.3                 | 11.1                  | 24.9                    | 17.9                              |
| 50  | 1.51     | 3000       | 9.3                 | 14.3                  | 29.5                    | 23.7                              |
| 50  | 3.14     | 6000       | 11.0                | 17.1                  | 34.8                    | 29.9                              |
| 50  | 6.28     | 6000       | 12.9                | 20.4                  | 43.2                    | 39.2                              |

<sup>a</sup> Here  $N$  is the chain length,  $T_t$  is the total duration of the run (after equilibration),  $\langle d \rangle$  is the average height of the monomers from the cylinder surface,  $\langle d_e \rangle$  is the average height of the free ends from the cylinder surface,  $\langle R_G^2 \rangle$  is the average radius of gyration of the chains squared, and  $\langle R_{G_{\perp}}^2 \rangle$  is the sum of the contributions to the average radius of gyration squared in the directions perpendicular to the line.



**Figure 1.** Typical configurations of systems of 50 chains of length  $N = 50$ , grafted on cylinders of radii  $R$  at a surface coverage  $\rho_a$ : (a)  $R = 20$ ,  $\rho_a = 0.03$ , (b)  $R = 5$ ,  $\rho_a = 0.03$ , and (c)  $R = 5$ ,  $\rho_a = 0.1$ . The chains are projected on the plane perpendicular to the cylinder axis.

picture contains 50 chains so that, depending on the surface coverage and radius of the cylinder, the length  $l_x$  of the cylinder over which the projection is made is different. Note that as  $R$  decreases  $h$  increases as the chains become more densely packed near the surface. In order to describe the structure of the layers quantitatively, we calculated several averaged quantities. The average thickness of the brush is defined by

$$\langle d \rangle = \langle (y_i^2 + z_i^2)^{1/2} - R \rangle \quad (4)$$

with  $(x, y, z)$  being the coordinates of monomer  $i$  with respect to an origin on the axis of the cylinder, which in our case coincides with the  $x$  axis. Here  $\langle \dots \rangle$  stands for an average over all the monomers in the system as well as a configuration average taken every 1000 time steps. The average height of the free ends,  $\langle d_e \rangle$ , is given by eq 4 except that the average is restricted to the free end monomers. The mean-squared radius of gyration of the chains is given by

$$\langle R_G^2 \rangle = \frac{1}{N} \left\langle \sum_{j=1}^N (\vec{r}_{ij} - \vec{r}_{j,cm})^2 \right\rangle \quad (5)$$

Here  $\vec{r}_{ij}$  is the coordinate vector of monomer  $i$  of chain  $j$

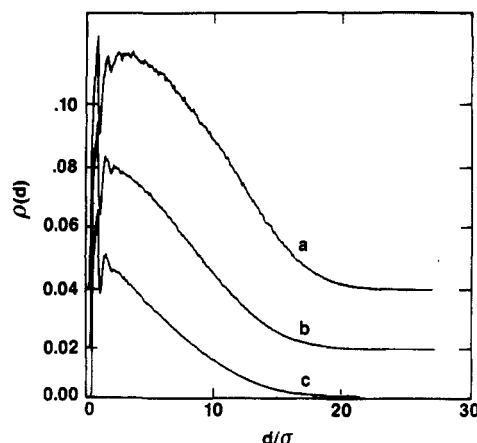


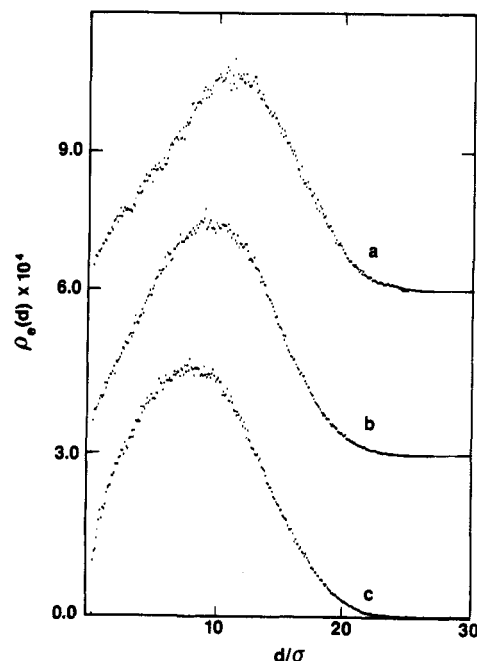
**Figure 2.** Monomer density profile for polymers of length  $N = 50$  at  $\rho_a = 0.03$  grafted onto a cylinder of radii (a)  $R = 20$ , (b)  $R = 5$ , and (c)  $R = 2$ . Each curve is shifted vertically with respect to the previous one by 0.02 for clarity.

and  $\bar{r}_{j,cm}$  is the center of mass position of chain  $j$ . We also calculated the contribution to  $\langle R_G^2 \rangle$  from the  $y$  and  $z$  directions, denoted as  $\langle R_{G,yz}^2 \rangle$ . Table I shows the results for these quantities for all the cases studied. For comparison, the relaxation times of the chains, calculated by using a procedure described in ref 8 are approximately  $100\tau$  for the systems with  $N = 50$ , of order  $400\tau$  for systems with  $N = 100$ , and  $900\tau$  for the one with  $N = 150$ .

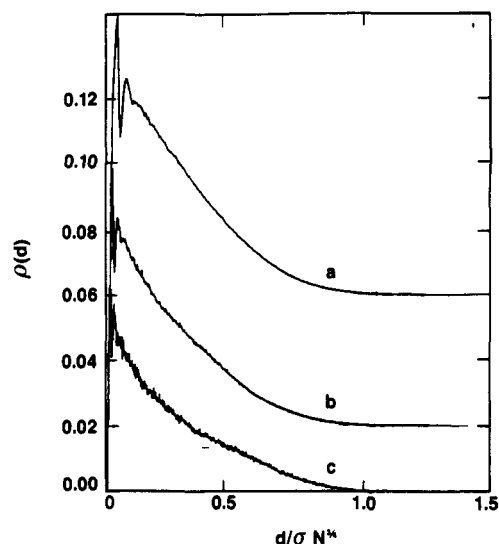
We also determined the local monomer density,  $\rho(d)$ , and the density of the free ends,  $\rho_e(d)$ . By the symmetry of the system, these quantities are only a function of the distance from the grafting surface,  $d = (y^2 + z^2)^{1/2} - R$ . They are normalized so that the volume integrals of  $\rho(d)$  and  $\rho_e(d)$  over the simulation box give  $NM$  and  $M$ , respectively. Figure 2 shows the monomer density profiles for chains of length  $N = 50$  at a surface coverage of  $\rho_a = 0.03$  grafted onto cylinders of radius  $R = 20, 5$ , and  $2$ . In a previous study,<sup>8</sup> we had found that flat brushes at this surface coverage are satisfactorily described by the self-consistent-field theory of Milner et al.,<sup>5</sup> with a parabolic density profile. The profile for  $R = 20$  is practically indistinguishable from that of a flat plate.<sup>8</sup> As the radius decreases, the density profile changes its shape, going over to one with steeper increase near the surface. The maximum density that is attained somewhere close to the surface also decreases. Figure 3 shows the density of the free ends for these cases. We find that this density is nonzero everywhere within the brush, including the region near the surface. In fact, we find that an increasingly larger fraction of the ends are found near the surface as the radius decreases. The average distance of the free ends from the surface, as shown in Table I decreases with decreasing  $R$ . We do not see any indication of a dead zone for these cases.

Figure 4 shows the monomer density for  $R = 2$  and  $\rho_a = 0.3$  with varying chain length. We find that the maximum density is quite insensitive to  $N$ . As all three curves can be put onto approximately the same horizontal scaling the distance by  $N^{3/4}$ , these systems are close to the limit of polymers grafted on a line that will be further discussed in the next section. As seen from Figure 5 for the end density profiles for these cases, we again find that there is no indication of a dead zone in this limit either.

Increasing the surface coverage beyond 0.03, we begin to see some indication that there is a region near the surface where the end density seems to vanish. Figure 6 shows the end density for two systems with  $N = 50$  and  $R = 5$  but much higher surface coverage,  $\rho_a = 0.1$  and  $0.2$ .



**Figure 3.** Density of the free ends as a function the height from the surface of the cylinder for the three cases presented in Figure 2. Curves a and b are shifted vertically and scaled by a factor of 0.25 and 0.5, respectively, in order to put them on the same scale.



**Figure 4.** Monomer density profile as a function of the height from the cylinder for polymers of length (a)  $N = 50$ , (b)  $N = 100$ , and (c)  $N = 150$ , grafted on a cylinder of radius  $R = 2$  at a surface coverage of  $\rho_a = 0.03$ . The curves are shifted vertically for clarity.  $d$  is scaled by  $N^{3/4}$ , appropriate for the limiting case of  $R/\langle d \rangle \rightarrow 0$ , where  $R/\langle d \rangle$  is the average thickness of the polymer layer.

Especially for the latter case, the end density seems to vanish close to the surface. However, comparing this with the end density profile for the flat brush at the same surface coverage,<sup>8</sup> we find a similar behavior there as well, due to the high densities attained near the surface. We therefore conclude that the vanishing of the end density near  $d = 0$  is not a consequence of the finite curvature but is rather due to the enhanced monomer density near the surface, which excludes all monomers from the surface that are more than a few chemical units from the attached end.

#### IV. Polymers Grafted on a Line

An interesting limit of the cylindrical brushes is obtained when the radius of the cylinder is reduced to zero. A

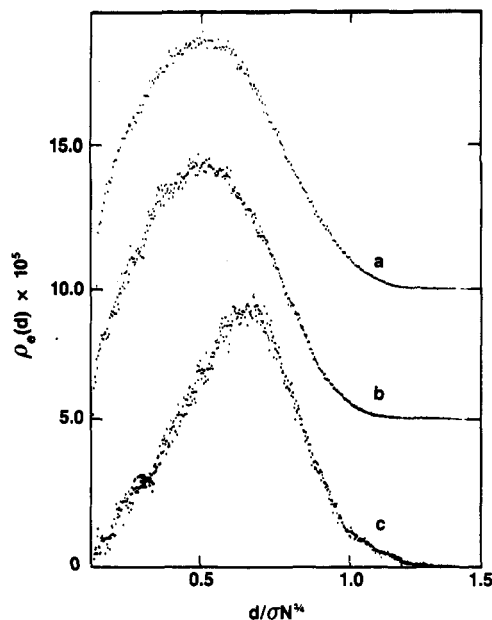


**Figure 5.** Density of the free ends as a function the height from the surface of the cylinder for the three cases presented in Figure 4. Curves a and b are shifted vertically and scaled by a factor of 0.2 and 0.5, respectively, to put them on the same scale.

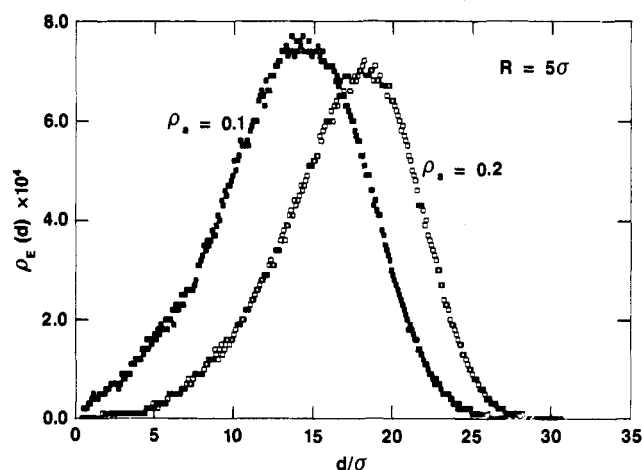


**Figure 6.** Density of the free ends for chains of length  $N = 50$  grafted on a cylinder of radius  $R = 5$  at surface coverages of (a)  $\rho_s = 0.1$  and (b)  $\rho_s = 0.2$ .

straightforward application of the scaling theory<sup>16,18</sup> leads to the result that the monomer density varies with the distance  $d$  from the line as  $\rho(d) \propto \rho_l^{2/3} d^{-1/3}$ . Here  $\rho_l$  is the number of chains per unit length. The average height (or any other measure of the size) of the chains scales with the chain length and linear density as  $\langle d \rangle \propto N^{3/4} \rho_l^{1/4}$ .

Figure 7 shows a typical configuration for polymers grafted onto a line for three different linear densities,  $\rho_l = 0.38, 3.14$ , and  $6.28$ . All three systems consist of 50 chains with  $N = 50$ . The polymers are projected on the plane perpendicular to the grafting line. With comparison of these pictures with those of star polymers,<sup>17</sup> the chains are much more stretched due to the constraints imposed by neighboring chains on the line. Results for some of the properties of the four systems studied are summarized in Table II. The average thickness,  $\langle d \rangle$ , of the chains is consistent with the scaling prediction. In Figure 8 we plot the monomer density profile for these systems on a double-logarithmic scale. We find that the region near the grafting line exhibits local ordering and that the density drops sharply near the outer end of the chains. The intermediate region, however, is dominated by a power law decay of the

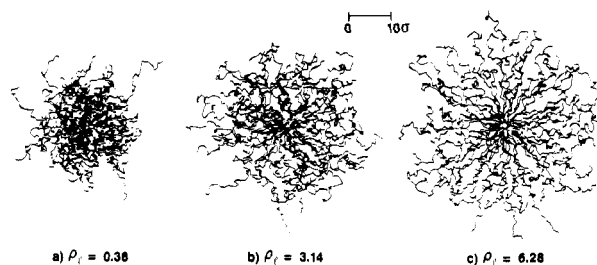


**Figure 7.** Typical configurations of systems of 50 chains of length  $N = 50$ , end-grafted onto a line density (a)  $\rho_l = 0.38$ , (b)  $\rho_l = 3.14$ , and (c)  $\rho_l = 6.28$ . The chains are projected on the plane perpendicular to the grafting line.

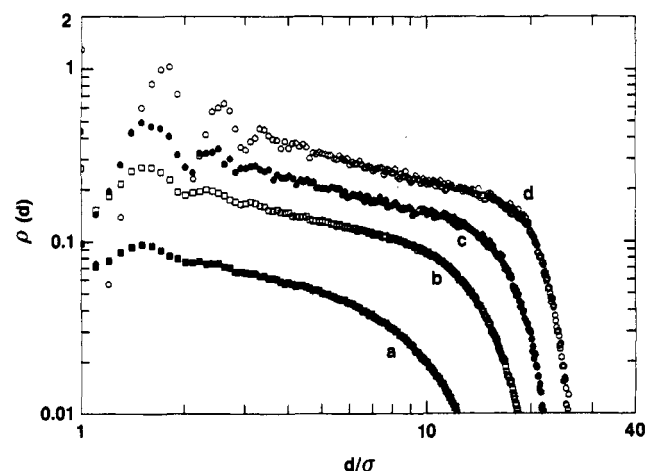


**Figure 8.** Monomer density profile vs height on a log-log scale for polymers of length  $N = 50$  end-grafted onto a line at a line density of (a)  $\rho_l = 0.38$ , (b)  $\rho_l = 1.51$ , (c)  $\rho_l = 3.14$ , and (d)  $\rho_l = 6.28$ .

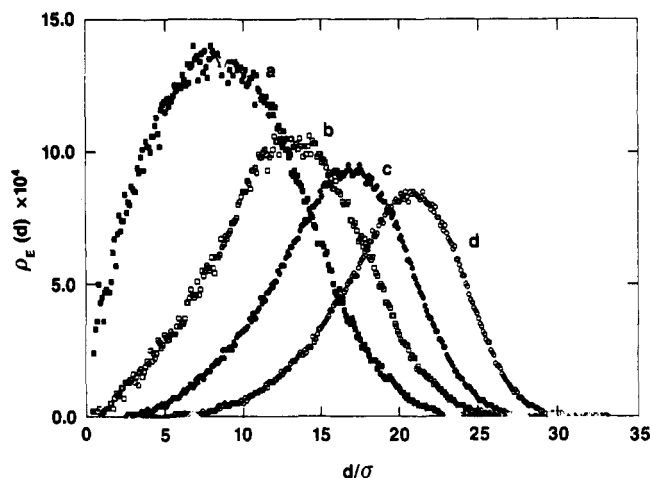


**Figure 9.** Density of the free ends as a function the height from the grafting line for the four cases presented in Figure 8.

density. In this region, we find that the exponent is closer to  $1/2$  than the expected value of  $2/3$ . However, since the fitting region is only about 1 decade in the distance  $d$ , we do not attach much significance to this difference.

Addressing again the question of the existence of a dead zone for the free ends, we show in Figure 9 this density scaled by  $\rho_l$  for the four cases. This time we find a definite region, especially for the higher densities, from where the free ends are excluded.

## V. Summary

We have simulated systems of polymer chains grafted on cylindrical surfaces under good solvent conditions, with

the ratio of the cylinder radius,  $R$ , to the typical polymer size,  $h$ , varying between order unity and zero. We find that when this ratio is finite, the free ends of the chains have a finite probability of being anywhere within the brush. This is contrary to the recent suggestion of Milner and Witten<sup>15</sup> and Ball et al.<sup>14</sup> that these ends should be excluded from a region near the cylinder surface even in a good solvent. While this case has not been worked out in detail, Ball et al.<sup>14</sup> find that, for the melt case, which we have not considered here, a dead zone near the surface does exist with a width proportional to  $h \exp(-R/h)$ . In the limit that the radius of the cylinder vanishes, we find that our results are reasonably well described by scaling theory. In this limit, where the radius of curvature,  $R$ , of the surface becomes much smaller than the height of the chain, we do find evidence for a dead zone for the free ends when the linear density  $\rho_e$  also becomes quite large. However, the origin of this dead zone is simply due to steric packing constraints. The density near the surface (or line) is simply too large for monomers many chemical units away from the grafted end to approach the surface.

**Acknowledgment.** We thank J. Marko, S. T. Milner, and T. A. Witten for helpful discussions. M.M. is a recipient of the Chaim Weizmann postdoctoral fellowship.

## References and Notes

- (1) Alexander, S. *J. Phys. (Paris)* **1977**, *38*, 983.
- (2) de Gennes, P.-G. *Macromolecules* **1980**, *13*, 1069.
- (3) de Gennes, P.-G. *C. R. Acad. Sci. Paris* **1985**, *300*, 839.
- (4) Cosgrove, T.; Heath, T.; van Lent, B.; Leermakers, F.; Scheutjens, J. *Macromolecules* **1987**, *20*, 1692.
- (5) Milner, S. T.; Witten, T. A.; Cates, M. E. *Macromolecules* **1988**, *21*, 2610.
- (6) Milner, S. T.; Witten, T. A.; Cates, M. E. *Europhys. Lett.* **1988**, *5*, 413.
- (7) Semenov, A. N. *Sov. Phys. JETP* **1985**, *61*, 733 (*Zh. Eksp. Teor. Fiz.* **1985**, *88*, 1242).
- (8) Murat, M.; Grest, G. S. *Macromolecules* **1989**, *22*, 4054.
- (9) Chakrabarti, A.; Toral, R. *Macromolecules* **1990**, *23*, 2016.
- (10) Skvortsov, A. M.; Pavlushkov, I. V.; Gurbonov, A. A. *Polymer Sci. USSR* **1988**, *30*, 487.
- (11) Cosgrove, T. *J. Chem. Soc., Faraday Trans.* **1990**, *86*, 1323.
- (12) Hadziannou, G.; Patel, S.; Granick, S.; Tirrell, M. *J. Am. Chem. Soc.* **1986**, *108*, 2869.
- (13) Taunton, H. J.; Toprakcioglu, C.; Fetters, L. J.; Klein, J. *Macromolecules* **1990**, *23*, 571.
- (14) Ball, R. C.; Marko, J. F.; Milner, S. T.; Witten, T. A. *Macromolecules* **1991**, *24*, 693.
- (15) Milner, S. T.; Witten, T. A. *J. Phys. (Paris)* **1988**, *49*, 1951.
- (16) Daoud, M.; Cotton, J. P. *J. Phys. (Paris)* **1982**, *43*, 531.
- (17) Grest, G. S.; Kremer, K.; Milner, S. T.; Witten, T. A. *Macromolecules* **1989**, *22*, 1904.
- (18) Birshtein, T. M.; Borisov, O. V.; Zhulina, Ye. B.; Khokhlov, A. R.; Yurasova, T. A. *Polym. Sci. USSR* **1987**, *29*, 1293.
- (19) Grest, G. S.; Kremer, K. *Phys. Rev. A* **1986**, *33*, 3628.
- (20) Kremer, K.; Grest, G. S.; Carmesin, I. *Phys. Rev. Lett.* **1988**, *61*, 566.
- (21) Kremer, K.; Grest, G. S. *J. Chem. Phys.* **1990**, *92*, 5057.
- (22) Grest, G. S.; Murat, M. *J. Phys. (Paris)* **1990**, *51*, 1415.